

Single molecule tracking of the molecular mobility in thinning liquid films on thermally grown SiO₂.

Daniela Täuber, Mario Heidernätsch, Michael Bauer, Günter Radons, Jörg Schuster and Christian von Borczyskowski.

Technische Universität Chemnitz, Institut für Physik, Germany.

Daniela Täuber
TU Chemnitz, Institut für Physik,
Reichenhainer Str. 70,
D-09126 Chemnitz, Germany
daniela.taeuber@physik.tu-chemnitz.de

keywords: near surface diffusion, liquid layering, thermal diffusion, single molecule tracking, square displacements, ultrathin liquid films.

Abstract

Diffusion coefficients obtained from weighted mean square displacements along probe molecule trajectories within ultrathin liquid TEHOS films show a correlation with film thickness. By studying cumulative distributions obtained with a time resolution of 20 ms, we could show that the diffusion is heterogeneous within our liquid films which consist of a few molecular layers only. We detected two components of the diffusion process, a slower and a faster one. Thinning of the film due to evaporation caused a slowdown of the whole diffusion process. But this resulted not from a slowdown in the two contributing components itself. Instead their relative contributions changed in favor for the slow component. We conclude that there is no pronounced difference in the diffusion coefficients attributed to the molecular layers 3 to 5 vertically above the substrate, but with the loss of upper layers along with the thinning process the concentration of probe molecules in the near surface region containing only one or two molecular layers is increased.

1. Introduction

Dynamics in liquid molecular films in the thickness range of few nanometers close to solid interfaces have gained importance since technologies have been scaled down to the nanometer range. In that case the molecular film topology and dynamics deviate from that within bulk liquids. E.g. liquid layering structures of a few layers close to the liquid-solid interface have been detected by evaporation experiments [1] and X-ray studies [2]. Additionally, in such thin layers interface properties have a crucial impact e.g. via processes of adsorption/desorption at the surface [3,4,5]. In case of thin liquid films the film thickness may vary in time due to evaporation processes [1]. This will have impact on

both dynamic and static film properties [6]. The vast interest in molecular biology has also contributed to the importance of studying such interfaces, since biomolecules usually operate in liquids close to interfaces with membranes.

Optical methods are a matter of choice for investigation of living systems because of their non-invasive character. Spatially resolved single molecule experiments are superior to ensemble methods due to their sensitivity in revealing heterogeneities of the molecular environment of e.g. probe molecules in ultrathin liquid films [7,8,9]. Usually fluorescent dye molecules with high photostabilities as well as with high quantum yields such as rhodamines are used to probe the spatial distribution of static and/or dynamic properties of liquid films or confined liquids [10,11] via microscope techniques such as confocal or wide field microscopy. Here we study the mobility of Rhodamine B in an ultrathin film of the organic liquid tetrakis-2-ethylhexoxy-silane (TEHOS) on a silicon wafer with a 100 nm thick thermally grown oxide layer at room temperature.

In previous investigations in our group on these ultrathin liquid films [8,9] we have used the method described by Saxton [12], in order to calculate diffusion coefficients for each detected dye trajectory from weighted mean square displacements (msd) along that trajectory. The disadvantage of using msd is that it is an averaging method. While information on single molecules exploring heterogeneous environments may readily be achieved, only their time average will be gained. This may already conceal or obscure any intrinsic heterogeneity of the investigated system [13,14,15]. On the other hand thermal diffusion on the microscopic scale is a stochastic process, which needs a considerably large amount of data to achieve reliable relations with macroscopic observables. A different approach to get information on a system by single molecule tracking is therefore to sample large numbers of steps at time intervals of constant length and to investigate distributions of them [16]. This is not similar to an ensemble method, since the distributions of those steps may still display complex relations between the microscopic steps and macroscopic observables. One promising approach is using cumulative distributions of square displacements for fixed time intervals (logs) [17]. Here we report such cumulative distributions for a set of measurements during the evaporation of TEHOS (thinning process) over several days. We compare data obtained from the later approach to those obtained from determination of diffusion coefficients D_{msd} by mean square displacements (Saxton [12]). We will discuss the origin of the distribution of all these data in relation to the properties of ultrathin films and of the interface.

2. Experimental and data evaluation methods

An ultrathin liquid film of TEHOS (tetrakis-2-ethylhexoxy-silane, Aldrich) was prepared by dipcoating a silicon wafer with a 100 nm thick thermally grown oxide layer (ZfM, TU Chemnitz) in a solution of a few % TEHOS in hexane. Beforehand the substrate had carefully been cleaned in Piranha solution for 30

min. This yielded a TEHOS film with a thickness of a few nm, which we measured by ellipsometry. TEHOS is a viscous liquid with a sufficiently low evaporation pressure to assure a stable film thickness during a single experiment lasting about one hour. The effective molecular diameter is about 1 nm which slightly varies due to intrinsic configurations [18]. Previous studies on film thinning report that the TEHOS layer closest to the substrate is 0.6 nm thick, followed by at least four layers of about 1 nm thickness each [1].

As a fluorescent probe for single molecule tracking experiments Rhodamine B (RhB) had been added to the TEHOS in a nanomolar concentration. The samples were investigated with a home built wide field microscope [19], containing a 100x0.9 NA (Zeiss Epiplan Neofluar) objective, and a lens (focal length 250 nm) for imaging onto a frame transfer EMCCD camera (iXon DU885, Andor Technologies). Dye molecules were excited through the same objective using the 514 nm line of an argon-krypton ion laser. Since the focal area of our microscope is larger than the film thickness, we image the projection of the thermal diffusion of the dyes in the plane parallel to the sample surface (two-dimensional projection of trajectories). Measurements were performed every one to three days within the thinning period of the liquid film. Fluorescence has been sampled with an integration time $\Delta t = 20$ ms (exposure time of the sample during one frame). Each such frame was immediately digitalized and transferred to a computer while the fluorescence signal for the next frame was collected on the camera chip (frame transfer technique, camera software: Andor Solis). In this way we recorded sequences of 5,000 frames. For each measurement ten such sequences were acquired, resulting in 50,000 frames in total. Within each frame the fluorescence of a dye molecule will be collected during the corresponding exposure time thus resulting in diffraction limited spots smeared out by the underlying diffusion.

For each spot the center of intensity was determined to obtain the average position of the dye molecule during the exposure time of the frame. With a tracking procedure developed in our group [20] we traced the obtained positions of dye molecules within the recorded sequences of 5,000 frames. For each detected trajectory a diffusion coefficient was calculated via mean square displacements [12]. Additionally square displacements (sd) of the dye positions between succeeding frames were calculated from all trajectories in a sequence. We then excluded those squared displacements, which within our positioning accuracy belonged to immobile molecules. To do so we set for each measurement a threshold $M(\text{SNR}, \Delta t)$ linearly depending on the signal to noise ratio (SNR) [21]. Above this $M(\text{SNR}, \Delta t)$ any sd would within 98% probability be related to a mobile molecule. From those remaining sd we calculated cumulative stepsize distributions as was described recently [17]. But different to [17] we rescaled our cumulative stepsize distributions by dividing the obtained sd by $4\Delta t$. Since the sd themselves resemble averages (during exposure time), and

since macroscopic diffusion coefficients are linked to averaged square displacements by the Einstein Smoluchowski Equation (in two dimensions):

$$D = \lim_{\Delta t \rightarrow \infty} \frac{\langle sd(\Delta t) \rangle}{4\Delta t} \quad (1)$$

dividing the sd by $4\Delta t$ will render $sd/4\Delta t = di$, which we name diffusivity. Thus we denote our cumulative distributions as $C(di, \Delta t)$.

The average of the sd at the right hand in eq. (1) will render the macroscopic diffusion coefficient D only at infinite times. Practically this will be realized, when the dye molecules had enough time to sample all different environments within the sample. But here we are not interested in the macroscopic diffusion coefficient of the system, since it is by definition at infinite times related to homogeneous diffusion. Instead we want to reveal heterogeneities within (vertically) different layers of the sample. In particular we want to know whether the detected layering structure of the liquid will be correlated to varying diffusion coefficients. To proceed we need short observation time intervals and we will have to sample a large number of diffusivities. The related distribution of di will then provide information about heterogeneities within the sample.

3. Results and Discussion

Since our samples usually exhibited a change in the distribution of observed diffusion coefficients within the first 50 hours (which may be due to some variations in surface chemistry), we will focus only on the later measurements where the distribution of diffusion coefficients clearly is correlated to the film thickness. Figure 1 shows for each set of measurements (50,000 frames) the diffusion coefficients D_{msd} determined from the individual trajectories. The diagrams in Figure 1a contain only those trajectories, which exceeded an area of $1.3 \mu\text{m}^2$. Their time length varies from 0.3 s (15 frames) to 29.4 s. D_{msd} varies between $0.1 \mu\text{m}^2/\text{s}$ and $4.1 \mu\text{m}^2/\text{s}$ resulting in broad distributions, showing a pronounced dependence on varying sample conditions e.g. film thickness and adsorption sites at the liquid-solid interface [6]. The distribution depends on the 7 - 294 hours waiting time after sample preparation. Within the first 50 hours the distributions of D_{msd} broaden and their medians shift to larger values. We will report on this part of our long time observations elsewhere. Here we will focus on times longer than 150 hours, where the distributions narrow again while the medians are decreasing. We believe that this decrease is correlated to the thinning of the film via evaporation of TEHOS. Figure 2 shows the medians depending on film thickness. The measurement after 294 h for the 3.2 nm thin film yielded only 22 trajectories which fulfilled the criterion for the distributions in Figure 1a, therefore its median is given in brackets.

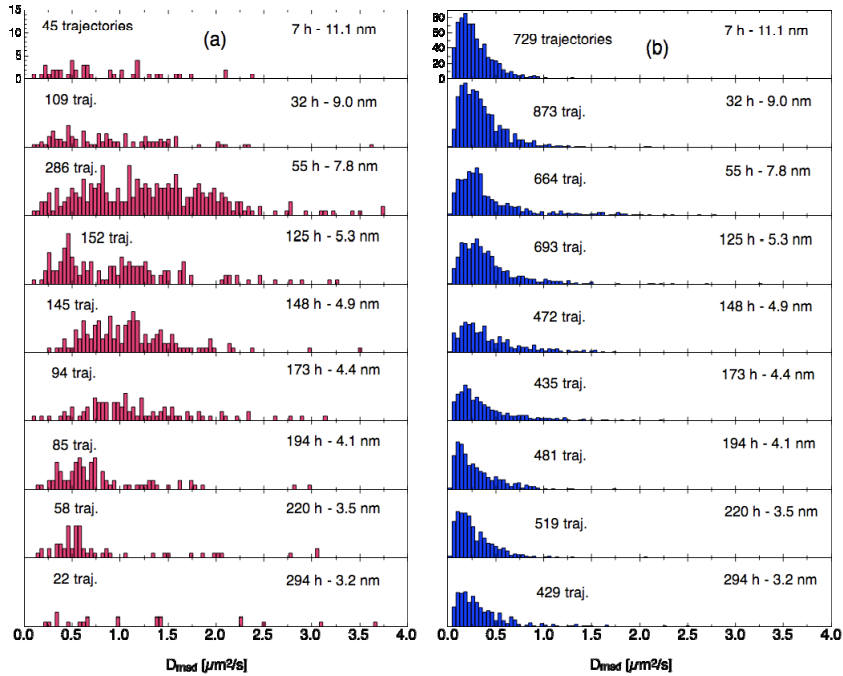


Fig. 1: Long time observation of RhB in thinning TEHOS film. Distribution of D_{msd} for (a) trajectories exceeding a lateral area of $1.3 \mu\text{m}^2$ (and time length ≥ 0.3 s); (b) all trajectories, i.e. no criterion on area (and time length ≥ 0.6 s).

For comparison Figure 1b shows the distributions for all detected trajectories (with time lengths ≥ 0.6 s, the longest lasted for 65,3 s). This does also include predominantly or even completely immobile molecules. The number of trajectories of these distributions is on one hand related to slightly varying experimental conditions, particularly to photobleaching during sample alignment. On the other hand immobile molecules will be bleached faster than mobile ones, thus the fewer detected trajectories for the later recordings could be related to a larger amount of immobile dye molecules. The medians and width of those distributions also change within time, but less significantly (see Figure 2 for the medians). Now the question arises, whether any vertical heterogeneity within the film, i.e. distinguishable diffusion coefficients for different molecular layers, is responsible for this change. For example at

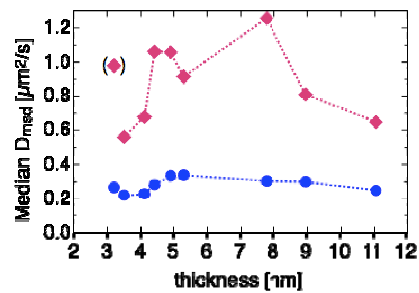


Fig. 2: Median D_{msd} of distributions of Fig. 1a (squares) and 1b (circles).

148 h the film thickness is 4.9 nm, corresponding to 5 complete molecular layers and one incomplete one. On the other hand the film thickness of 3.2 nm at 294 h corresponds to less than four complete layers.

For each set of recordings we have determined the related film thickness via ellipsometry at a given time after sample preparation. The corresponding values of film thickness are indicated in Figures 1, 3 and 5.

As stated above calculating diffusion coefficients from mean square displacements is an averaging method which may conceal heterogeneities. To overcome this limitation we collected cumulative distributions $C(d_i, \Delta t)$ of diffusivities d_i for films with a thickness in the range from 4.9 nm to 3.2 nm, see Figure 3. If the dye mobilities within the exposure time of 20 ms were homogeneously distributed, the $C(d_i, 20 \text{ ms})$ should display a mono-exponential dependence of d_i resulting in straight lines in the semi-log plots of Figure 3. But the shapes of all obtained $C(d_i, 20 \text{ ms})$ clearly deviate from a mono-exponential behavior. However, they could be fitted with a bi-exponential function (using Levenberg-Marquardt-Algorithm) according to

$$C(d_i, \Delta t) = a_1 \exp(-d_i/D_1) + a_2 \exp(-d_i/D_2) \quad (2)$$

This results in two diffusion coefficients D_1 and D_2 (determined for $\Delta t = 20 \text{ ms}$) revealing a heterogeneity of our system at least at times shorter than 20 ms. Figure 4a shows D_1 and D_2 as a function of film thickness. For each set of recordings the values for the ten sequences (each one consisting of 5,000 frames) are shown. The lines connect the respective mean values. In Figure 4b the relative (mean) amplitudes a_2 are shown as a function of film thickness.

Since we have excluded immobile molecules from the $C(d_i, \Delta t)$ distributions, the observation of two diffusion coefficients can not be explained only by the process of ad-/desorption at the interface and an otherwise homogeneous diffusion in the liquid, but the liquid films contain at least two distinguishable physical diffusion coefficients which we name D_{slow} and D_{fast} . The residual times of the dye molecules in the corresponding regions within the films are long enough in respect to our exposure time ($\Delta t = 20 \text{ ms}$) to reveal this heterogeneity. If they were too short, the dye would have enough time to sample all regions, thus leading to homogeneous diffusion within the 20 ms exposure time. However we cannot address D_1 as D_{slow} and D_2 as D_{fast} unless we can show that the average residual times within the corresponding regions will exceed our exposure time. Our investigations addressing this question will be reported elsewhere.

We believe that the observed D_1 and D_2 are characteristic compositions of the underlying physical processes within our exposure times. Here we will outline one likely scenario where D_1 and D_{slow} resp. D_2 and D_{fast} will not match: D_{fast} could be bulk diffusion, D_{slow} could either be some kind of surface diffusion, where the molecule may glide on the surface e.g. via silanol bridging [22], or a slowdown of diffusion in the liquid layer(s) close to the solid interface [8]. We address both of as „near surface“ diffusion. We calculated the bulk diffusion coefficient of TEHOS by the Stokes-Einstein-Relation to be $72 \mu\text{m}^2/\text{s}$. This is in good agreement with NMR-measurements yielding a value of $77 \mu\text{m}^2/\text{s}$ at room temperature [23].

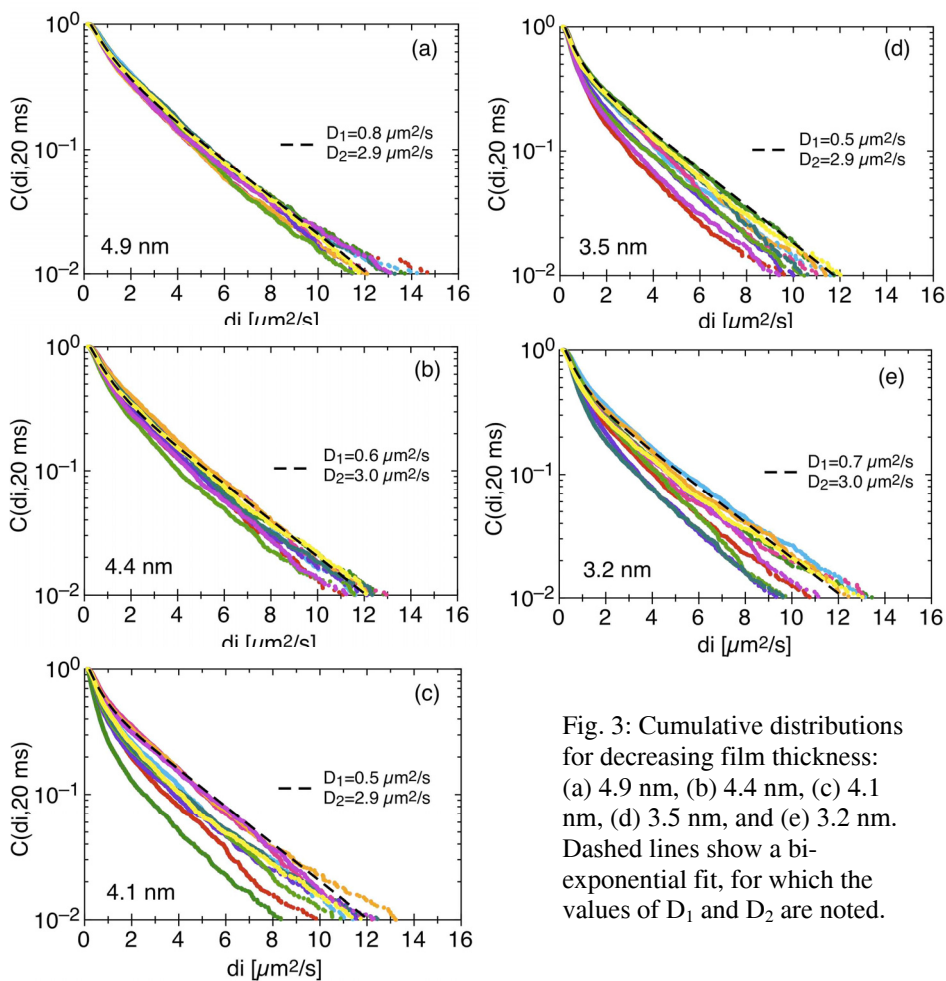


Fig. 3: Cumulative distributions for decreasing film thickness: (a) 4.9 nm, (b) 4.4 nm, (c) 4.1 nm, (d) 3.5 nm, and (e) 3.2 nm. Dashed lines show a bi-exponential fit, for which the values of D_1 and D_2 are noted.

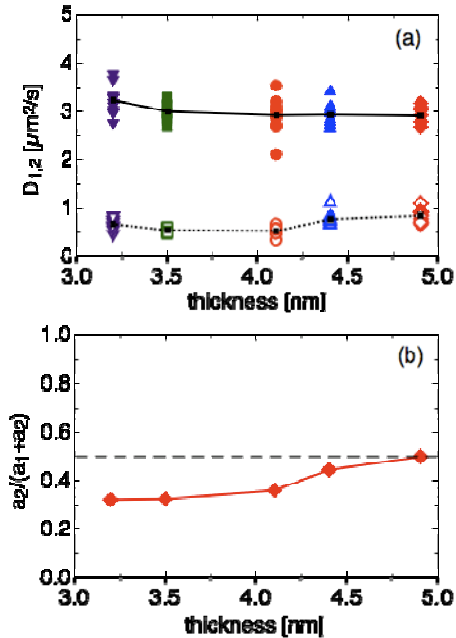


Fig. 4: (a) Diffusion coefficients D_1 (open symbols) and D_2 (filled symbols) from bi-exponential fits to each distribution $C(d_i, \Delta t)$ in Fig.3. Mean values of D_1 resp. D_2 are connected by lines. (b) Mean values of fraction of amplitude a_2 for those fits. Error bars denote standard deviations.

experimental conditions have led to variations in the detection limit for different sets of measurements, thus causing the fluctuations of D_1 seen in Figure 3b. At this fast timescale we are not able to distinguish between very slow diffusion and complete immobility.

One important result is the nearly constant average value for D_2 ($3.0 \pm 0.1 \mu\text{m}^2/\text{s}$) during film thinning from 4.9 nm to 3.2 nm. The seemingly slight increase at 3.2 nm stems from two less quality fits which yielded somewhat unreasonable high values for D_2 . But the overall quality of the bi-exponential fits did only slightly deviate from those for 4.9 nm, as can be seen from the corresponding plots of their residuals in Figure 5a and b. Nevertheless this shows that there is no pronounced difference between the diffusion coefficients D_{fast} in the upper layer of the 3.2 nm thin film and in those layers present in the 4.9 nm thin film, which were lost during evaporation. The 3.2 nm thin film only contains three

Rhodamine B is of similar size as the liquid TEHOS molecules. Furthermore it is highly diluted (nanomolar concentration). Therefore it is convenient to use the bulk value of the liquid for RhB as well. Because particle tracking methods use during the exposure time geometrically averaged positions (2-dimensional Gaussian fits to the detected spots), the obtained diffusion coefficients will be different from the real diffusion coefficients [21,24]. In our detection scheme exposure times and cycle times (inverse frame rates) are identical within 1 ms. The diffusion coefficients therefore result in only 2/3 of the real diffusion coefficients. In case of the bulk diffusion $D = 75 \mu\text{m}^2/\text{s}$ will be reduced to $50 \mu\text{m}^2/\text{s}$. Therefore a mean residual time of about 1 ms within the region of bulk diffusion would lead to values for $D_2(20 \text{ ms})$ of about $3 \mu\text{m}^2/\text{s}$ as has been obtained from our fits (see Figure 4a). To interpret D_1 is more complicated, since it is naturally correlated with the detection limits for mobile molecules. The slightly different

complete molecular layers and an incomplete fourth one, whereas at 4.9 nm the film still contains five complete molecular layers. Therefore there can be only minor changes within the values of the diffusion coefficients of the third to fifth molecular layer.

Furthermore from Figure 4b we can see a decrease in the amplitude a_2 of the faster component D_2 which shows that with decreasing film thickness the concentration of dye molecules tends to become higher within the near surface region. Thus the change in shape of the distributions of D_{msd} of the 4 thinnest films in Figure 1a is not due to a loss of layers containing faster diffusion coefficients, but due to a higher probability of finding the molecules in the near surface region. Our previous measurements of films with a thickness below 2 nm revealed hardly any trajectory which fulfilled the threshold criteria (area $> 1.3 \mu\text{m}^2$) that has been applied for the trajectories used for the distributions shown in Figure 1a. This might point towards either a pronounced slowdown of the diffusion within the two molecular layers closest to the substrate, or it also could be due to a higher adsorption probability (and thus reduction of mobility) at the solid-liquid interface.

4. Conclusions

Cumulative distributions of diffusivities obtained from single molecule tracking at exposure times in the range of 20 ms with an optical wide field microscope provide a powerful tool to study the heterogeneities of molecular motion in ultrathin (≤ 10 nm) films at solid-liquid interfaces. From film thinning experiments we conclude that no significant slowdown of the diffusion occurs down to the third molecular layer (three molecular diameters above the solid substrate). On the other hand the dye concentration in the near surface region (containing the one or two molecular layers closest to the substrate) increases for thinner films. Thus the change of the distributions of diffusion coefficients calculated from weighted mean square displacements (D_{msd}) can be explained

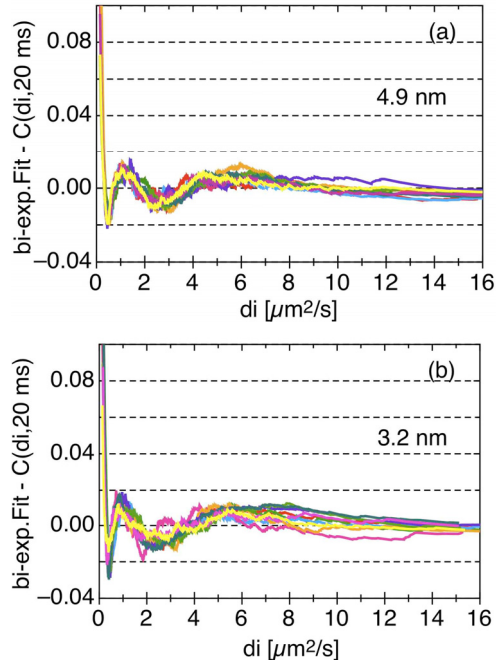


Fig. 5: Fitting residuals for two comparative bi-exponential fits for (a) 4.9 nm (Fig.3.a), and (b) 3.2 nm (Fig.3.e) thick films.

by the increased presence of probe molecules in layers close to the substrate. Access to even shorter exposure times will reveal whether there are still slight variations between diffusion coefficients in different upper molecular layers. On the other hand variations of the dye-substrate interactions will reveal more information about the nature and the magnitude of the slow diffusion in the near surface region.

We thank the German Science Foundation for funding (DFG-FOR 877, From local constraints to macroscopic transport), and we thank Prof. Dr. D. Zahn for the permission to use his ellipsometer.

References

- [1] M.L. Forcada, M. Mate, *Nature* 363 (1993) 527-529.
- [2] C.-J. Yu, A. G. Richter, A. Datta, M. K. Durbin, P. Dutta, *Phys. Rev. Lett.* 82 (1999) 2326-2329.
- [3] H. Graaf, M. Vieluf, C. von Borczyskowski, *Nanotechnology* 18 (2007) 265306.
- [4] F. Dinelli, J.-F. Moulin, M. A. Loi, E. Da Como, M. Massi, M. Murgia, M. Muccini, F. Biscarini, J. Wie, P. Kingshott, *J. Phys. Chem. B* 110 (2006) 258-263.
- [5] M.J. Saxton, *Biophys. J.* 70 (1996) 1250-1262.
- [6] D. Täuber, J. Schuster, M. Heidernätsch, M. Bauer, G. Radons, C. von Borczyskowski, *Diffusion Fundamentals* (2009) accepted.
- [7] J. Schuster, F. Cichos, C. von Borczyskowski, *J. Phys. Chem. A* 106 (2002) 5403-5406.
- [8] J. Schuster, F. Cichos, C. von Borczyskowski, *Eur. Phys. J. E* 12 (2003) 019.
- [9] J. Schuster, F. Cichos, C. von Borczyskowski, *Eur. Polym. J.* 40 (2004) 993-999.
- [10] A. Schob, F. Cichos, *Diffusion Fundamentals* 2 (2005) 76.
- [11] C. Jung, J. Kirstein, B. Platschek, T. Bein, M. Budde, I. Frank, K. Müllen, J. Michaelis C. Bräuchle, *J. Am. Chem. Soc.* 130 (2008) 1638-1648.
- [12] M.J. Saxton, *Biophys. J.* 72 (1997) 1744-1753.
- [13] M. Heidernätsch, Masterarbeit, TU Chemnitz 2009.
- [14] A. Kammerer, F. Höfling, T. Franosch, *Eur. Phys. Lett.* 4 (2008) 66002.
- [15] F. Höfling, T. Franosch, E. Frey, *Phys. Rev. Lett.* 96 (2006) 165901.
- [16] M. Bauer, M. Heidernätsch, D. Täuber, J. Schuster, C. von Borczyskowski, G. Radons, *Diffusion Fundamentals* (2009) accepted.
- [17] C. Hellriegel, J. Kirstein, C. Bräuchle, V. Latour, T. Pigot, R. Olivier, S. Lacombe, R. Brown, V. Guieu, T. Payaraste, A. Izquierdo, P. Mocho, *J. Phys. Chem. B* 108 (2004) 14699-709.
- [18] S. Vilette, M. P. Valignat, A. M. Cazbat, L. Jullien, F. Tiberg, *Langmuir* 12 (1996) 825-830.
- [19] B. Schulz, Diplomarbeit, TU Chemnitz, 2009.
- [20] J. Schuster, Dissertation, TU Chemnitz, 2002.

- [21] T. Savin, P.S. Doyle, *Biophys. J.* 88 (2005) 623-639.
- [22] A. Honciuc, A.W. Harant, D.K. Schwartz, *Langmuir* 24 (2008) 6562-6566.
- [23] R. Valiullin, private communication.
- [24] D. Montiel, H. Cang, H. Yang, *J. Phys. Chem. B.* 110 (2006) 19763-19770.